論文 / 著書情報
Article / Book Information

論題(和文)	
Title(English)	Ionic Transport Phenomena in Glass Under the Field-Assisted Ion Exchange
著者(和文)	矢野哲司, 李在高, 船曳富士, 柴田 修一
Authors(English)	Tetsuji Yano, Jaeho Lee, Fuji Funabiki, Shuichi Shibata
出典(和文)	, Vol. , No. , pp. O-07-003
Citation(English)	XX International Congress on Glass, Kyoto, Japan, Vol. , No. , pp. O-07-003
発行日 / Pub. date	2004,

IONIC TRANSPORT PHENOMENA IN GLASS UNDER THE FIELD-ASSISTED ION EXCHANGE

Tetsuji Yano*, Jaeho Lee, Fuji Funabiki & Shuichi Shibata
Department of Chemistry and Materials Science, Tokyo Institute of Technology, Ookayama, Meguro-ku, Tokyo 152-8550, Japan
tetsuji@ceram.ttiech.ac.jp

Eiji Ichikura
Research Center, Asahi Glass Co., Ltd, Hazawa-cho, Kanagawa-ku, Yokohama 221-8755, Japan

Yuichi Kuroki, Mikio Ueki, & Tsunehiko Sugawara
Display Company, Asahi Glass Co., Ltd, Yuraku-cho, Chiyoda-ku, Tokyo 100-8405, Japan

Ionic transport phenomena in mixed alkali silicate glasses under the field-assisted ion-exchange treatments were investigated. The glass samples with various Na:K ratio were prepared based on the commercial glasses for CRT. Their ionic conductivities and the transport numbers of these glasses were measured. The ionic conductivities showed the typical mixed alkali ion effect (MAE) at Na/(Na+K)=36%, at which the transport numbers of g_{Na} and γ_K had a crossover to alternate the main charge carrier of the ionic conduction in the glass. The differences in the transport number and the conductivity between the ion-exchanged layer and the mother glass were found to be very important to understand the mechanism of the formation of the ion-exchanged layer by the field-assisted ion exchange. The characteristic features of the concentration profiles of the ion-exchanged surface by EPMA could be well explained by using these parameters.

(Key words: field-assisted ion exchange, ionic conductivity, transport number, mixed alkali ion effect)

1. Introduction

Coexistence of more than 2 kinds of alkali ions in the glass is well known to show various characteristic properties of glass [1,2]. When the molar ratio of alkali oxides in oxide glass system is changed, non-linear changes of the glass properties are induced. This well-known 'mixed alkali ions effect' (MAE) has been utilized to give characteristic properties to the glasses. High chemical durability, high electrical resistivity, and high browning toughness to the irradiation of high energy particles can be listed as the typical properties [2]. The interactions between alkali ions in the glass are still one of the important issues to be investigated in the field of glass science and technology. Various kinds of mixed alkali glass systems have been examined by many researchers and the interaction models [3-6] have been reported in the literatures. As reviewed in the recent paper by Ingram [7], however, the details of the MAE have not been well understood.

The MAE of the ionic conductivity is the most popular phenomenon. Most of the investigated mixed alkali glasses were prepared by melt-quenching method, where the concerned alkali ion pairs were already incorporated into the glasses. Ion-exchange treatment is an alternative process to incorporate second alkali ions into the glasses. In detail, the ion-exchange treatment can be classified into two categories. One is the dipping method. The glass specimen is dipped into the molten salt and the mobile ions in the glass are replaced by the second ions from the molten salt. Its main process is the counter-diffusion driven by the thermal energy and the concentration gradient. Another one is the field-assisted ion-exchange method. This utilizes the Coulomb force in addition to the thermal energy, and differs completely from the dipping method from the point of view of the movement of mobile ions in the glass; the alkali ions, for instance, move towards the same direction not only in the vicinity of the glass surface but also over the whole glasses under the electric field. Therefore, we have to pay much attention to the glass conductivity as well as the ion-exchange layer.

In this work, the field-assisted ion exchange was applied to silicate glasses with various Na:K ratio in order to understand the mechanism of the ion-exchange process. The ionic conductivities and the transport numbers of the glasses were measured. Combining these results with the EPMA profile analysis, the characteristic transport phenomena of the field-assisted ion exchange were discussed.

2. Experimental

Glass Sample Preparation

The composition of the examined glasses were determined based on the commercial mixed alkali glass used for CRT: $66SiO_2$-8PbO-5CaO-3.5MgO-3.5Al_2O_3-$x$$Na_2O$-(14-$x$)$K_2O$ (in mol%). The model glass C corresponds to the commercial glass composition. The glass samples were prepared by the melt-quenching method. The obtained annealed glasses were cut and polished into the dimension of 40 x 40 x 1 and 50 x 50 x 10 in mm for the electrical conductivity measurement and the field-assisted ion-exchange treatment, respectively. The characteristic physical constants of these samples are listed in Table 1.

Table 1. Characteristic properties of the glass samples.

Glass	Model A	Model B	Model C	Model D	Model E	Model F
x	14	11	8	5	3	0
Na/(Na+K)=R (%)	100	79	57	36	21	0
Density	3.038	3.014	2.999	2.984	2.978	2.957
Strain point T_s (^{o}C)	455	442	447	461	473	509

Electrical Conductivity Measurement

The electrical conductivities of the glass samples were measured by AC 2-electrodes method. The Au electrodes with 30 mm in diameter were coated on the both sides of the glass samples by sputtering method. The samples were heated in the electric furnace, and the temperature was changed from 300 to 450^{o}C by 50^{o}C step and controlled within ±2^{o}C. The AC electric field with the frequency f from 10Hz to 10MHz was applied between the 2 electrodes, and the impedance $\mathbf{Z}$ was collected as a function of the frequency and temperature. DC conductivity at the respective temperature was obtained from the Cole-Cole plot and/or $\mathrm{Re}[\mathbf{Z}]$-f plot as a value extrapolated at $f \rightarrow 0$.

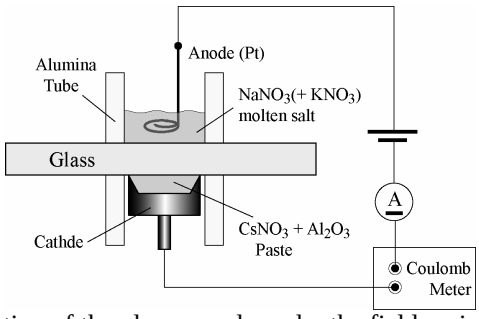

Fig. 1 Schematic illustration of the glass sample under the field-assisted ion-exchange treatment. The electric furnace is not drawn for simplicity.

Field-Assisted Ion-Exchange Treatment and Transport-Number Measurement

Field-assisted ion-exchange treatments were carried out on the glass samples of 50 x 50 x 10 in mm. The set-up for the field-assisted ion exchange of the glass sample, the electrodes, the molten salts and the electric circuit was illustrated in Fig. 1. The glass plate was sandwiched by a couple of alumina tubes with O.D.=28mm. KNO_3 (and/or $NaNO_3$) salt was melted inside the upper alumina tube, and contact with the glass surface with a certain area, where the alumina tube was pressed closely on the glass surface to hold the molten salt. The anode electrode (Pt wire) was immersed in the molten salt. Al_2O_3 paste containing $CsNO_3$ melt on the stainless plate (the cathode electrode) was pressed onto the bottom glass surface inside the bottom alumina tube to make a close contact between them. These were heated in the electric furnace up to the strain point T_s or T_s-25^{o}C of the respective glass (see Table 1), and DC-voltage 300V or 100V was applied between the electrodes. The current conducting the circuit was monitored by the current meter and the total charge was counted by the coulomb meter. When the total charge reached to the settled values (12, 24, 48 and 96C), the DC-voltage supplier and

the electric furnace were immediately turned off, and the sample glasses were cooled to the room temperature. The Al_2O_3 paste on the cathode electrode was analyzed after the treatment by the induction coupled plasma (ICP) spectroscopy, and the fractions of the extracted cations from the glass samples were obtained.

3. Results

Physical Properties of Glass Samples

The density and the strain point of the glass samples are plotted in Fig. 2 as a function of R (=Na/Na+K %). Strain point T_s shows non-linear change with the increasing R. The minimum of T_s was found around R=75-80%. Density plots also show a simple linear increase with the increasing R position. The increasing Na^+ fraction increases the packing density of the glasses to chancel well the effect of the decreasing mass.

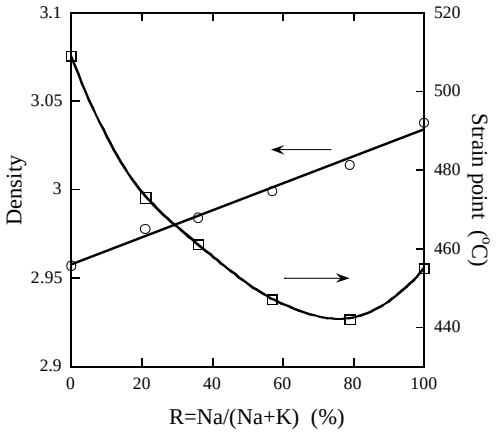

Fig. 2 Plots of the density and the strain point T_s of the glass samples against R (=Na/Na+K). The lines were drawn as guides for eyes only.

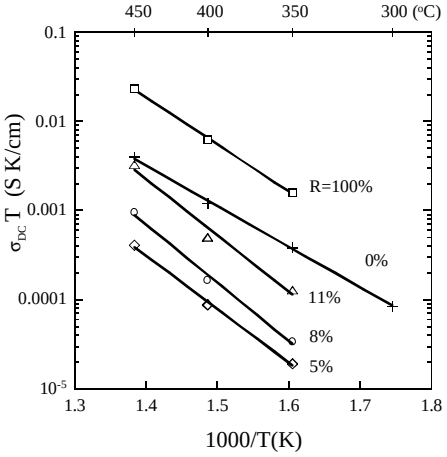

Fig. 3 Arrhenius plots of $\sigma_{DC}T$ of the glass samples. The lines were drawn by the least square fitting procedures.

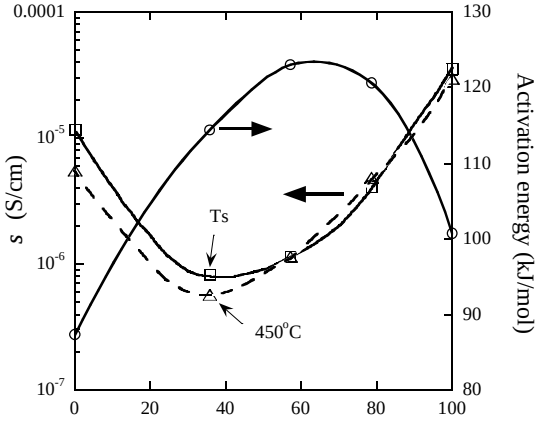

Fig. 4 Plots of DC conductivites σ_{DC} at T_s of the respective glass samples and at 450°C(=T_s of the model C glass), and the activation energy for the ionic conduction as a fiction of R.

Ionic Conductivity and Activation Energy

The measured DC conductivities σ_{DC} of the glass samples are plotted in Fig. 3. All the glasses show Arrhenius-type behavior. The model A glass sample has the largest σ_{DC} among the examined glasses. The plots could be fitted well by the least square method and the activation energy values were derived from the slopes. They are plotted in Fig. 4 with the ionic conductivities at T_s and 450°C. The typical mixed alkali ion effects (MAE) were observed. The conductivity minimum was found around R=36%, while the activation energy maximum was around R=60%. The latter maximum point is given at almost the same R of the minimum of the strain point in Fig. 2

Ionic Transport Number

Figure 5 shows the fraction of the extracted Na^+ and K^+ ions from the model C glass (the commercial CRT glass) into the cathode paste as a function of the total conducting charge Q. ICP analysis did not detect other cation like Pb^{2+}, Ca^{2+} etc. This means that the detected Na^+ and K^+ ions were electrically extracted from the bottom glass surface. In addition, these fractions depend only on the charge Q, but neither on the anode salt nor on the applied DC voltage. This means that the analyzed Na^+ and K^+ fractions represent the transport number g of cations in the glass. At a small Q region, the transport number of Na^+ ions (g_{Na}) is almost unity, but gradually decreases with increasing Q. At Q>48C, g_{Na} and g_K become constant. Taking into account the fact that R (=Na^+ fraction) of this glass is 57%, the contribution of Na^+ ions to the ionic conduction is quite large.

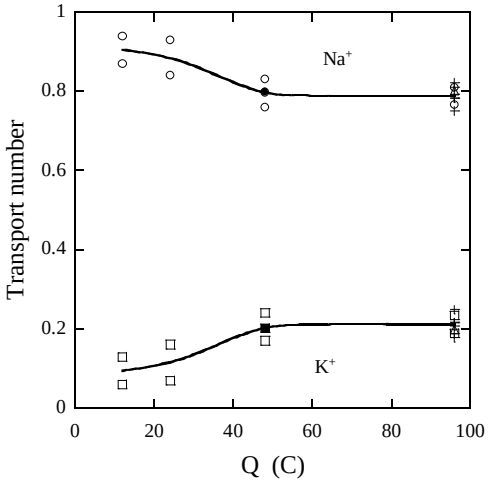

Fig. 5 Plots of the transport numbers of Na^+ and K^+ in the model C glass against the total charge Q. Open circle and square: KNO_3 anode salt and 300V, filled square: $NaNO_3$ salt and 300V, plus: $NaNO_3$+KNO_3 salt and 300V, open triangle: KNO_3 salt and 100V.

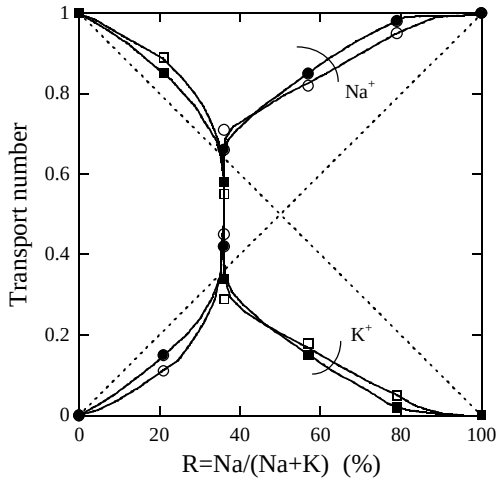

Fig. 6 Plots of the transport numbers of Na^+ and K^+ ions as a function of R in the glass samples. Circle symbol: γ_{Na}, square symbol: γ_K, open symbol: measured at T_s-25°C, closed symbol: measured at T_s.

Figure 6 shows the plots of g_{Na} and g_K as a function of R of the glass samples. All the plots were obtained at Q=48 or 96C. The g_{Na}, for instance, is much smaller than g_K and increases gradually with increasing R in the glass samples. At R=36%, it increases very steeply and has a crossover with the plot of g_K. At R>36 region, the g_{Na} exceeds 0.7, and are plotted separately from the concentration fraction (shown by broken lines in the figure). The crossover points (R=36%) is well corresponding to the conductivity minimum, but not to the maximum of the activation energy or the minimum of T_s (see Figs. 2 and 4).

4. Discussion

The effects of s_{DC} and g on the formation of the ion-excahnged layer

The MAE of the ionic conductivity was found at R=30-40%. When the field-assisted ion exchange on the glass with R=57% is considered to form K^+ layer on the glass surface (chemical tempering), the composition of the glass surface has to change from R=57 to 0% by passing through the strong MAE region. Kuroki *et al*. [8] reported the detailed EPMA analysis results of the field-assisted ion-exchanged layers formed on the same glass samples. The observed characteristic features of the concentration profiles in the ion-exchanged layer were (1) the step function-type profiles of the ion-excahnge frontier surface (R>36), (2) the exponential function-type profiles of the residual Na^+ ions, and (3) the decrease of the total alkali oxide concentration in the ion-exchanged layer and its strong dependence on R of the mother glass.

The formation of the step function-type concentration profile is the most important feature of the field-assisted ion exchange [9]. Differing from the thermal diffusion ion exchnage, the alkali ions in the glass move towards the same direction to form a new composition region behind the ion-exchange frontier. In most cases, the ionic conductivity of this new region differs from that of the mother glass, and this conductivity difference brings about the characteristic progress of the ion exchange. EPMA

results reveal that this ion-exchange frontier region has certain thikness of the order of micrometer. In this frontier region, Na^+ ions concentration decreases very steeply and fastly below 30% of the total alkali ions by the replacement with K^+ ions. As shown in Fig. 6, the transport number, g_{Na}, becomes smaller than g_K at R<36%, and within this thinn frontier regions, the mobility of Na^+ ions is reduced largely. Figure 6 also says that the starting R of the mother glass in 36<R≤100 would not affect the residual Na^+ concentration, because the crossover point of g between Na^+ and K^+ is caused at the same Na:K ratio. This reduced g_{Na} in the K^+-rich ion-excahnged layer would be an origin to leave traces of Na^+ as an exponential function-type profile.

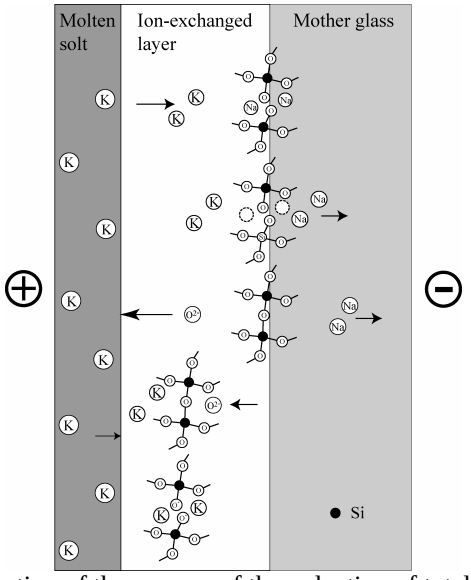

Fig. 7 Schematic illustration of the process of the reduction of total alkali oxide in the ion-exchanged layer.

On the other hand, the thinn ion-exchange frontier region is considered to be important to induce the decrease of the total alkali oxide concentration (and NBO concentration) in the ion-exchanged layer. EPMA analysis [15] reveals that about 14% of the total alkali oxide was reduced in the ion-exchanged layer in the model B glass. σ_{DC} in Fig. 4 shows that the model B glass (R=79%) has an about 10 times large σ_{DC} of the minimum σ_{DC} at R=36%. This large difference in σ_{DC} would leave vacant alkali ion sites (NBO sites) at the ion-exchange frontier region. Figure 7 schematically illustrates one of the possible mechanisms of the reducing alkali oxides in the ion-excahnged layer. When a pair of Na^+ ion sites in the ion-exchange frontier region are considered (the top species), the electric field enforces Na^+ ions to move towards the cathode side leaving a couple of vacant sites (second species). When the condictivity difference between the mother glass and the ion-exchanged layer is small, the diffusing K^+ ions occupy these vacant sites simultaneously, and the ion exchange frontier advances toward the cathode side. However, the increase of R of the mother glass increases the conductivity difference between two regions, and also increases the probability (or time) of these vacant site unoccupied. Since an NBO has a negative charge, Coulomb force would attract NBOs to the anode side, and the recombination between NBOs according to the following reaction would proceed (the third species in Fig. 7),

$$\equiv Si-O^- + {}^-O-Si\equiv \rightarrow \equiv Si-O-Si\equiv + O^{2-} \quad (1)$$

The increasing R of the mother glass increases this recombination process, while the decrease of R (the increase of K^+ ratio) of the mother glass would reduce the probability of the above reaction, because the above reaction requires a pair of vacant sites at the same time.

The induced oxide anion O^{2-} would diffuse towards the anode side [10]. Since K^+ ions are continuously supplied from the anode molten salt, the following reaction might quench the further diffusion of O^{2-} (the forth species in Fig. 7).

$$2K^+ + \equiv Si-O-Si\equiv + O^{2-} \rightarrow \equiv Si-O^-K^+ + K^+{}^-O-Si\equiv \quad (2)$$

However, Eq. (2) has to create certain free space to break Si-O-Si bonds and make a couple of K^+ sites. K^+ ions incorporation, on the other hand, induces high compressive stress in the ion-exchanged layer

and would suppress the quenching of the diffusion of O^{2-}. Therefore, the diffusion length of O^{2-} is considered to be long enough to go to the glass/molten salt interface. The large decrease of the total alkali oxide in the vicinity of the glass surface is considered to be caused by the above mechanism. O^{2-} diffusion in the ion-exchanged layer should be included to the contribution to the transport number and would affect the efficiency of the progress of the ion-exchanged layer.

Calculation of Thickness of Ion-Exchanged Layer

Finally, the dependence of the thickness of the ion-exchanged layer on R of the mother glasses is considered. From the above discussion, the thickness of ion-exchanged layer is considered to be defined by 3 factors; the transport number (factor 1), the amount of the residual Na^+ ions in the ion-exchanged layer (factor 2) and the transport of O^{2-} (factor 3). These factors can be quantitatively estimated, and then the thickness of the ion-exchanged layer can be calculated to compare with the observed one (from the EPMA analysis of the samples treated at T_s for 96C). Figure 8 plots the calculated thickness taking these factors into account. It is obvious that although there is a difference in the degree of the thickness from the observed ones, details of the dependence of the thickness on R can be well reproduced (compare the open circles with the closed circles). If the dependence of g on Q is also taken into account, the difference between the observed thickness and the calculated one would become small, and more precise estimation of the thickness of the ion-exchanged layer can be attained. In the process of the field-assisted ion exchange, the conduction parameters of all the systems are found to be indispensable for the design of the ion-exchange layer of the glass surface.

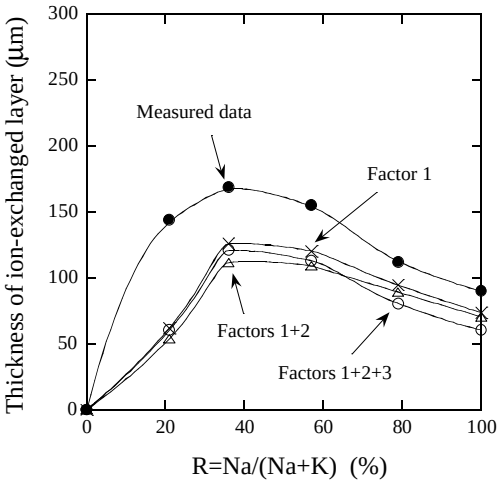

Fig. 8 Calculation of the thickness of the ion-exchanged layer thickness. The measured data are obtained by EPMA analysis on the samples treated at T_s for 96C.

References

[1] J. O. Isard, *J. Non-Cryst. Solids*, **1** (1969) 235-261.
[2] D. E. Day, *J. Non-Cryst. Solids*, **21** (1976) 343-372.
[3] W. C. LaCource, *J. Non-Cryst. Solids*, **95&96** (1987) 905-912.
[4] P. Mazzoldi and A. Miotello, *J. Non-Cryst. Solids*, **95&96** (1987) 897-904.
[5] A. Bunde, M. D. Ingram, P. Maass, *J. Non-Cryst. Solids*, **172-174** (1992) 1222-1236.
[6] P. Maass, A. Bunde and M. D. Ingram, *Phys. Rev. Lett.*, **68** (1992) 3064-3067.
[7] M. D. Ingram, J. E. Davidson and A. M. Coats, *Glastech. Ber. Glass Sci. Technol.*, **73** (2000) 89-104.
[8] Y. Kuroki, M. Ueki, T. Sugawara, E. Ichikura, T. Yano, J. Lee, F. Funabiki and S. Shibata, *appeared in this issue.*
[9] H. Ohta and M. Hara, *Yokyo-Kyokai-Shi*, **78** (1970) 158-164; *Rep. of Res. Lab., Asahi Glass Co. Ltd.*, **20** (1970) 15.
[10] D. E. Carlson, K. W. Hang and G. F. Stockdale, *J. Am. Ceram. Soc.*, **55** (1972) 337-341.